Solar photothermal conversion characteristics of hybrid nanofluids: an experimental and numerical study

Xin Jin[a], Guiping Lin[a], Aimen Zeiny[b,c], Haichuan Jin[a,*], Lizhan Bai[a], Dongsheng Wen[a,b,*]

[a]*Laboratory of Fundamental Science on Ergonomics and Environmental Control,* School of Aeronautic Science and Engineering, Beihang University, Beijing 100191, PR China

[b]School of Chemical and Process Engineering, University of Leeds, Leeds, LS2 9JT UK

[c]Department of Mechanical Engineering, Faculty of engineering, University of Kufa, Iraq

Abstract: In this work, the Fe_3O_4, Cu and Au with different concentrations and the hybrid nanofluids were prepared and characterized to enhance the solar photothermal conversion performance based on the direct absorption concept. An extensive experimental study was carried out with different sample nanofluids under a solar simulator. The experiment was first conducted with Au nanofluid in three cases to investigate the effect of different test conditions, and the test condition where the simulated sunlight was absorbed by the sample nanofluid only once with minimum heat loss to the surroundings was determined for later research. Based on the experimental results, below conclusions have been reached: 1) the solar energy absorption performance of nanofluids with plasmonic nanomaterials, i.e., Au or Cu, is much better than that of nanofluids with non-plasmonic nanomaterials, i.e., Fe_3O_4 and DI water, due to the effect of localized surface plasmon resonance; 2) the larger the concentration, the higher the solar energy absorption efficiency, but the increasing rate of the absorption efficiency slows down gradually with the increase of the concentration; 3) a numerical method to predict photothermal conversion efficiency of nanofluid under solar radiation has been proposed; 4) the novel idea of employing hybrid nanofluid to enhance the solar absorption performance has been experimentally and numerical validated, which can enhance the solar photothermal conversion when mixing two nanofluids with different absorption peaks, and there is an optimal mixing volume fraction for hybrid nanofluid.

Key words: solar energy; nanofluids; direct absorption; hybrid nanofluid; absorption efficiency

[*] Corresponding author, Email: jinhaichuan@buaa.edu.cn;

d.wen@buaa.edu.cn

Nomenclature

A	surface area exposed to solar radiation (m^2)
	absorbance (-)
a_n	Mie coefficient to compute the amplitudes of the scattered field (-)
b_n	Mie coefficient to compute the amplitudes of the scattered field (-)
c	specific heat capacity ($\mathrm{J/(kg \cdot K)}$)
c_p	specific heat capacity at constant pressure ($\mathrm{J/(kg \cdot K)}$)
D	particle diameter (m)
D_p	Petri dish diameter (m)
E	spectral emissive power ($\mathrm{W/m^3}$)
f_v	volume concentration (-)
I	radiative intensity ($\mathrm{W/m^2}$)
k	thermal conductivity ($\mathrm{W/(m \cdot K)}$)
k_f	imaginary part of the complex refractive index of the based fluid (-)
L	optical depth (m)
m	mass (kg)
	relative refractive index (-)
n	complex refractive index (-)
	order of accuracy
q	heat flux ($\mathrm{W/m^2}$)
Q	efficiency factor for Mie scattering (-)

T temperature (℃)

t time (s)

U uncertainty (-)

x characteristic size of nanoparticles (-)

Greek symbols

β extinction coefficient (m^{-1})

ε spectral emissivity (-)

η efficiency (-)

κ absorption coefficient (m^{-1})

λ wavelength of light in vacuum (m)

σ scattering coefficient (m^{-1})

Stefan-Boltzmann constant = $5.670\times10^{-8}\left(W/\left(m^2\cdot K^4\right)\right)$

ρ density (kg/m^3)

ψ_n spherical Bessel function of order n

ξ_n spherical Bessel function of order n

Superscripts

\- average value

$\rightarrow$ vector quantity

Subscripts

abs absorption

amb ambient

b black body

ext extinction

f fluid

η wavelength range

I	radiative intensity
n	nanoparticle
p	particle
sca	scattering
s	scattering
w	water
Abbreviations	
ABE	absorption efficiency
DASC	direct absorption solar collector
DI	deionized
PTE	photothermal conversion efficiency
RTE	radiative transfer equation
SAR	specific absorption rate
TC	thermocouple
SEM	scanning electron microscope
UV	ultraviolet

1. Introduction

With the rapid development of social economy and growth of world population, there is a growing demand on energy for today's world. At the same time, with diminishing availability of fossil fuels and increasing concerns on environmental pollution and global warming, to develop sustainable and renewable energy technologies, especially solar energy related, becomes extremely important in securing our energy future [1–3], which attracts the interests of many researchers worldwide.

However nowadays, the solar energy utilization efficiency is still relatively low, and there exist many challenges to overcome before realizing its efficient and widespread utilization. While for the solar thermal energy applications, the big challenge lies in the solar photothermal conversion efficiency. In recent decades, in order to enhance the solar photothermal conversion performance, nanoparticle-based direct absorption concept has been proposed, which makes use of nanoparticles dispersed in the base fluid to realize effective and efficient solar photothermal conversion, and the solar thermal energy is eventually stored in the base fluid through the heat transfer between the nanoparticles and the base fluid [4–6].

Comparing to traditional solar thermal collectors that absorb the solar energy first by an engineered solid surface, then transport it through the conduction and convection processes, in this novel concept, properly selected nanoparticles absorb the solar energy directly within the base fluid. Such an idea transfers the surface heat transfer limitation associated with conventional solar thermal collectors into volumetric absorption process, which can increase the solar energy absorption efficiency considerably by properly engineering the solar absorption spectrum at the nanoscale [7–14]. So far, big progress has been made in this area since this new concept was first proposed, and the solar energy absorption performance of a variety of nanomaterials has been investigated both experimentally and theoretically, which will be reviewed in brief below.

Otanicar et al. [15] compared the photo-thermal efficiencies of different nanofluids including carbon nanotubes, graphite and silver nanofluids. It is found that the optical absorption properties are affected by the nanoparticle material, structure, shape, size and volume fraction. An efficiency improvement of up to 5% in solar thermal collectors by using nanofluids as the absorption mechanism was experimentally demonstrated. Karami et al. [16] prepared alkaline functionalized carbon nanotubes (f-CNT)/water nanofluid as working fluid of low-temperature direct absorption solar collector, and characterized its dispersion stability, optical properties and thermal conductivity. Experimental results confirmed that f-CNT can raise the optical properties of the fluid due to improvement of the light extinction level even at low volume fractions. 150 ppm f-CNT increased the extinction coefficient of pure water by about 4.1 cm^{-1}. Significant enhancement of thermal conductivity (32.2%) was observed for 150 ppm f-CNT /water nanofluid. With these promising properties, this kind of nanofluid is very suitable for increasing the overall efficiency of direct absorption solar collectors. Zhang et al. [17] proposed and validated a novel idea of using plasmonic nanoparticles (PNP) to improve the solar photo-thermal conversion efficiency. Gold nanoparticle (GNP) was synthesized through an improved citrate-reduction method, which was used as an example to illustrate the photo-thermal conversion characteristics of PNPs under a solar simulator. The experimental results showed that GNP has the best photo-thermal conversion capability comparing to other reported nanomaterials. At the lowest particle concentration examined (i.e. 0.15 ppm), GNP increased the photo-thermal conversion efficiency of the base fluid by 20% and reached a specific absorption rate (SAR) of 10 kW/g. The photo-thermal conversion efficiency increased with increasing particle concentration, but the SAR showed a reverse trend. Filho et al. [18] investigated experimentally the photo-thermal conversion characteristics of one of the plasmonic nanoparticles, i.e. silver, under realistic conditions. Stable silver nanofluids were formulated through a high-pressure homogenizer, and the experiments were conducted continuously under sunlight on a rooftop for 10h. The results showed that silver nanoparticles had excellent photo-thermal conversion capability even under very low concentrations. Up to 144% enhancement in the stored thermal energy can be obtained at the peak temperature for a particle concentration of 6.5 ppm. Nearly constant initial specific absorption rate (SAR), 0.6 kW/g, was obtained for nanoparticle concentrations up to 6.5 ppm, but it decreased significantly at higher concentrations. He et al. [19] prepared Cu-H_2O nanofluids through the two-step method, and the transmittance of nanofluids over solar spectrum (250-2500 nm) was measured by the UV-Vis-NIR spectrophotometer based on integrating sphere principle. The factors influencing transmittance of nanofluids, such as particle size, mass fraction and optical path were investigated. The extinction coefficients measured experimentally were compared with the theoretical calculation. Meanwhile, the photo-thermal properties of nanofluids were also investigated. The experimental results showed that the transmittance of Cu-H_2O nanofluids was much less than that of deionized water, and decreased with increasing nanoparticle size, mass fraction and optical depth. The highest temperature of Cu-H_2O nanofluids (0.1wt.%) can increased up to 25.3% compared with deionized water. The good absorption ability of Cu-H_2O nanofluids for solar energy indicated that it is suitable for direct absorption solar thermal energy systems. Khullar et al. [20] conducted an experimental study which quantitatively compared a nanofluid-based volumetric system to a conventional surface absorption-based system employing a solar selective surface. The nanoparticle dispersions were amorphous carbon nanoparticles dispersed in ethylene glycol and multi-walled carbon nanotubes (MWCNTs) dispersed in distilled water. The study showed that the nanofluid-based volumetric absorption system could be more efficient. There was an optimum volume fraction at which the nanoparticle dispersion-based volumetric system performed the best. Additionally, it was also shown that higher stagnation temperatures were possible in the case of volumetric absorption system, which can be attributed to the cumulative effect of higher optical efficiency and the higher conversion efficiency of radiant energy into the thermal energy in the working fluid. To assess the efficiency of direct absorption solar collector with different nanoparticles, Zhang et al. [21] conducted an experimental study of the photo-thermal conversion characteristics of a number of nanoparticle dispersions including Au, Si, Fe_3O_4, Al_2O_3 and diamond under the same experimental setup. The results showed that comparing with the base fluid, the introduction of nanoparticles can increase the photo-thermal conversion efficiency significantly, and the efficiency increased in the order of Al_2O_3, diamond, (Fe_3O_4 and Si) and Au.

Ladjevardi et al. [22] investigated the application of graphite nanofluid in direct absorption solar collector by numerical simulation. Radiative transport equations along with mass, momentum and energy equations were solved together to simulate the operating characteristics of direct absorption solar collector. Different diameters and volume fractions of graphite nanoparticles were investigated. Moreover, for a proposed low-temperature solar collector, increase in outlet temperature, convective thermal losses, and costs were evaluated. Results of this study showed that by using graphite nanofluid with a volume fraction around 0.000025%, it would be possible to absorb more than 50% of incident irradiation energy by just about 0.0045 $/L increase in cost, while pure water solar collector can only absorb around 27% of incident irradiation energy. Luo et al. [23] established a simulation model of nanofluid solar collector based on direct absorption concept by solving the radiative transfer equations of particulate media and combining conduction and convection heat transfer equations. The system efficiency and temperature distribution were analyzed by considering the absorption and scattering of nanoparticles and the absorption of the matrix. The simulation results showed that the nanofluids improved the outlet temperature and the efficiency by 30-100 K and by 2-25% than the base fluid. The photo-thermal efficiency of 0.01% graphite nanofluid was 122.7% of that of a coating absorbing collector. The study indicated that nanofluids, even of very low content, had good absorption of solar radiation, and can improve the outlet temperature and system efficiency.

According to the review above, both theoretical and experimental studies confirm that the employment of nanoparticles can indeed enhance the absorption efficiency of solar thermal energy considerably based on the direct absorption concept. Currently, in most studies, only a single kind of nanoparticles was adopted. For each kind of nanoparticles, it only has strong absorption capability within a narrow solar spectrum. In order to further enhance the absorption efficiency, it is necessary to improve the solar absorption in the whole solar spectrum, and the application of hybrid nanofluids, i.e. a mixture of different kinds of nanoparticles with the solar absorption peak at different wavelengths dispersed into the base fluid, is a practically feasible method. For instance, Au nanoparticles have excellent solar absorption performance due to the effect of localized surface plasmon resonance, however, the wavelength corresponds to its solar absorption peak is around 520 nm, and its absorption capability becomes much worse when the solar wavelength is larger than 600nm. For Cu nanoparticles, the wavelength corresponds to its solar absorption peak is larger than 700nm, so it is expected to improve the solar absorption in the whole solar visible spectrum (390-760nm) by the application of Cu+Au hybrid nanofluids. In this paper, hybrid nanofluids of Fe_3O_4, Cu and Au were prepared and tested under solar simulator. The photothermal conversion efficiency was evaluated based on theoretical model. Meanwhile, numerical works and other relevant factors affecting the solar energy absorption performance of the nanofluids were also investigated and discussed.

2. Experimental setup and material

2.1 Preparation of nanofluids

In this work, Massart co-precipitation method was considered for the production of Fe_3O_4 nanoparticles according to the following reaction [24]:

$$FeCl_2 + 2\ FeCl_3 + 8NaOH \rightarrow Fe_3O_4 + 8NaCl + 4H_2O \quad (1)$$

Table 1 shows the concentration and temperature condition of several experiment runs. The concentration of other components was prepared based on chemical stoichiometry with Ferrous chloride.

Table 1. The condition of nanoparticle synthesis in different experiment runs.

Experimental	Ferrous chloride	Temperatur
1	0.01	22 ºC
2	0.05	22 ºC
3	0.1	22 ºC
4	0.01	70 ºC
5	0.05	70 ºC
6	0.1	70 ºC

The reverse microemulsion was prepared by mixing1 ml ionized water containing $FeCl_3$and $FeCl_2$ with a mixture of 8 ml cyclohexane, 0.2 g Span80-1.8 g Tween80 and 2 ml propyl alcohol for 1 hours under magnetic stirring. One ml of sodium hydroxide solution as the precursor was added drop wise to the reverse microemulsion during 10 minutes. The mixture was stirred over 4 hours to reach the equilibrium. A trial was performed without using any surfactant in the mixture to compare with the reverse microemulsion method. SEM image for Fe_3O_4 nanoparticles is shown in **Fig. 1**.

The Cu nanofluid was formulated through two step method, i.e. by dispersing a certain amount of commercial Cu nanoparticles into DI water with pre-determined volume. In this work, the Cu nanoparticles were purchased from the Sigma-Aldrich Corporation with a size range of 60-80 nm. In the preparation process, a certain amount of dispersing agent (tri-sodium citrate) was first blended with DI water, then the pH value of the tri-sodium citrate aqueous solution was adjusted to about 10.0 by the precise addition of NaOH solution. After that, a certain amount of Cu nanoparticles was blended with the tri-sodium citrate aqueous solution. The suspensions were stirred for 30 min by magnetic stirring apparatus and then sonicated for 30 min with an ultrasonic device. SEM image for Cu nanoparticles is shown in **Fig. 1**.

The Au nanofluid was formulated through simultaneous production and dispersion of the nanoparticles in situ, i.e. one step method. Au nanoparticles were synthesized by the citrate reduction method with the aid of magnetic stirring. In the synthesis process, a mixture of 50ml 5mM $HAuCl_4$ aqueous solution and 50ml 10 mM tri-sodium citrate aqueous solution was heated until boiling, and stirred by a magnetic blender. The pH value of the mixture was adjusted as 7.50 by the addition of NaOH solution with the concentration of 1.0M, and the production process lasted about three hours until the color of the solution changed to dark wine red. After that, Au nanofluid was purified by the membrane dialysis method. In this process, Au nanofluid was put in a membrane tube with pore size of 2-3 nm in diameter, which allows the smooth diffusion of ions but keeps the Au nanoparticles always inside the tube. The membrane tube was located in a beaker filled with DI water of 2000 ml and stirred by a magnetic stirrer. SEM image for gold nanoparticles is shown in **Fig. 1,** which clearly shows the morphology information: most of the Au nanoparticles with smaller sizes are spherical, while a majority of Au nanoparticles with larger sizes are oval, and the average size of the Au nanoparticles is around 20-30 nm.

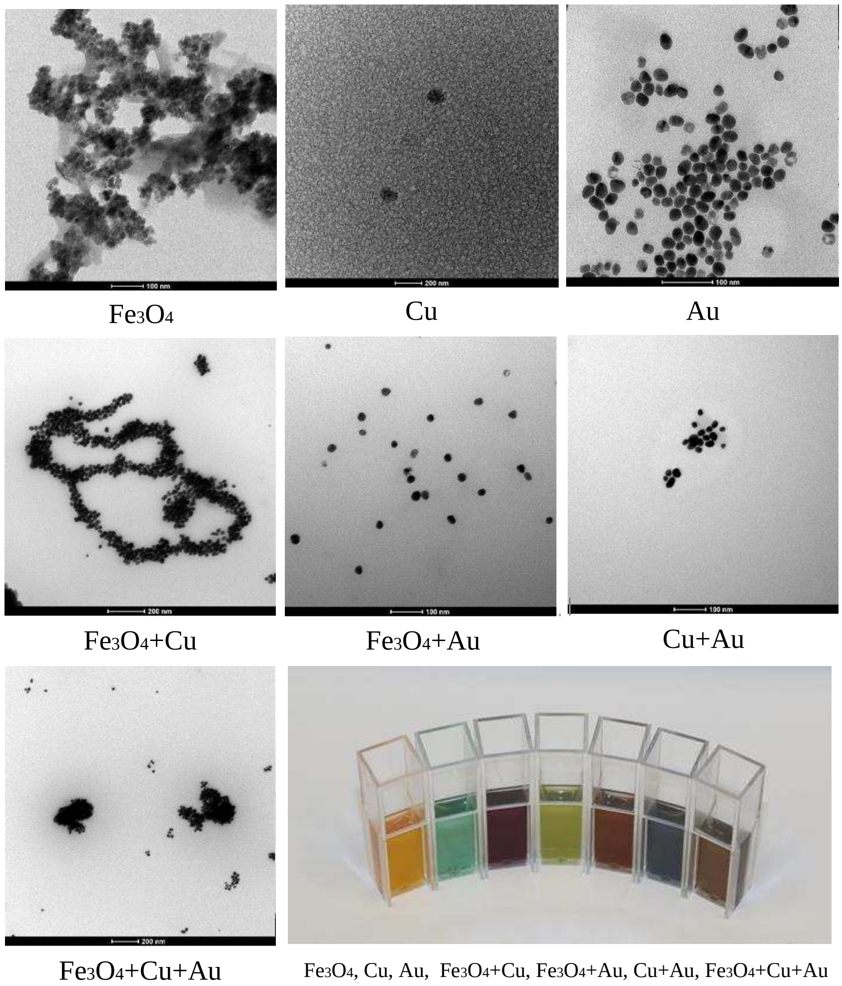

Fig. 1. SEM images and photo of different nanofluids

The synthesized nanofluids were put into an ultrasonic bath (ThermoFisher Scientific, FB11207) for 30 min. The concentration of the original nanofluid was determined as 330 ppm, 25ppm and 1500 ppm by the Atomic Absorption Spectroscopy (AAS), and the nanofluids with different concentrations were prepared by diluting the original ones with DI water. The Fe_3O_4, Cu and Au nanofluid with concentration of 200 ppm, 50 ppm and 6 ppm were selected for hybrid nanofluid preparation. The diluted solutions were processed by an Ultrasonic Cell Disruption (UCD) System (ThermoFisher Scientific, FB705) with 50% power for 2 hours. After that, the nanofluids were standing for 2 months and tested by a UV-spectrophotometer (Shimadzu UV-1800) to compare the changes in absorption. The difference of absorbance before and after standing for 2 months was less than 1%, which indicated that the nanofluids maintained good stability. The diluted Fe_3O_4, Cu and Au nanofluids (with concentration of 200 ppm, 50 ppm and 6 ppm, respectively) were mixed by the same volume of each one and processed by the UCD system for 3 hours. The SEM images can be seen in **Fig. 1**. The Fe_3O_4+Cu, Fe_3O_4+Au, Cu+Au and Fe_3O_4+Cu+Au hybrid nanofluids were tested by the UV-spectrophotometer, and the results showed that the deviation of absorbance maintained 1% in 1 week. In our previous research

[13,25], adding surfactant can significantly improve the stability of nanofluid. In order to improve the stability, dispersing agents of trisodium citrate (TSC) aqueous solution 0.5M and Gum-Arabic (GA) powder were added to the hybrid nanofluids at 2 vol% and 0.5 wt %, respectively. The deviation of absorbance maintained 1% in 3 months. However, to avoid the influence of surfactant on the absorption of solar energy, the hybrid nanofluids after UCD treatment and without any surfactant were selected for further experiments, and the experiments were conducted within 1 week after the UCD treatment. The optical property of nanofluid was characterized by a UV-spectrophotometer, as shown in **Fig. 2**. The Fe_3O_4 exhibits strong absorption from 300 nm to 450 nm, and no peak absorption is found. The peak absorption of Cu nanofluid is around 750 nm in spectrum. There is peak absorption at the wavelength of around 530 nm for Au nanofluid with concentration of 6 ppm, which is due to the strong Surface Plasma Resonance (SPR) effect in visible spectrum [26]. Many previous researches conclude that the strong absorption in visible light is the reason why gold nanofluid has high photothermal conversion efficiency. And seeking for nanofluid whose absorption shape in spectrum is similar with the shape of solar spectrum becomes popular when considering solar thermal harvesting [27,28]. However, the solar spectra emissive power exists from 200 nm to 3000 nm approximately, as shown in **Fig. 5**. Unilaterally considering the visible spectrum only may cause significant issues in calculating photothermal conversion efficiency. According to the Maxwell's equation [29], the scattering of nanofluid in this paper should be independent. As Cu and Au nanofluid have peak absorption in different wavelength of spectrum, the mixing of Cu and Au nanofluid makes the absorption more smooth in spectrum, as shown in **Fig. 2**. However, the mixing of Cu an Au nanofluid will dilute each other as the volume is the same. According to Beer's law [29], the absorbance of hybrid Cu-Au nanofluid should be the half of A_{Cu}+A_{Au} (A is the absorbance). That's the reason why the curve absorbance of Cu-Au nanofluid passes through the curve intersection of Cu and Au. The situation is the same for Fe_3O_4-Cu and Fe_3O_4-Au hybrid nanofluids. Further investigation into the absorbance will be discussed in **Section 4.5**.

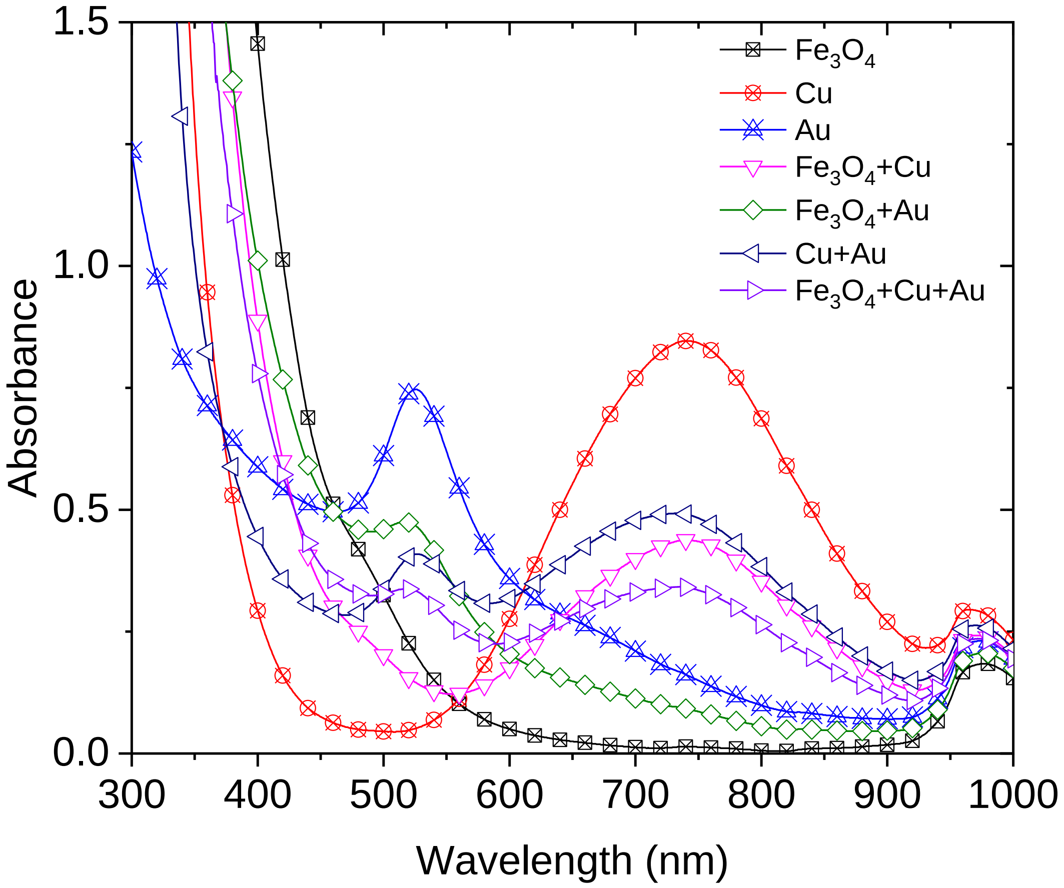

Fig. 2. The absorbance of different nanofluids

2.2 Experimental setup

Fig. 3 shows the experimental setup. In order to minimize the experimental uncertainties under direct sunlight, a solar simulator (Newport Co. Oriel Xenon Arc lamp, Model 94023A) was employed to simulate the real solar radiation. It provides a close spectral match to the real solar spectra. The performance parameters of the solar simulator are based on the ASTM standard (ASTM E927-05), including spectral match, non-uniformity of irradiance (5% maximum) and temporal instability (0.5% and 2.0% maximum for short- and long-term measurements, respectively). To minimize the temperature gradient inside the fluid, a thin layer of sample fluid (3 mm) was injected into a Petri dish with 3.5cm diameter, which was located on the bottom of an upside-down beaker in the center spot of the solar simulator. The solar radiation was maintained at approximately 980 W/m^2 (1.5AM) in all the experiments, and a uniform radiation from the solar simulator can be assumed. The center sample temperature was measured by a type K thermocouple (Sigma Cooperation, with uncertainty of ±0.1 °C), whose head was fixed on the bottom center of the Petri dish. The radiative intensity of solar simulator was measured by a radiative sensor (AccuPRO XP-2000) with a measurement uncertainty of 2.0%. The mass of nanofluid was measured by a digital balance (Ohaus Discovery Model

DV214c) with precision of ±0.0005 g. The inner diameter of the Petri dish was measure by micrometer with precision of ±5μm. The data was recorded in a PC though a data acquisition hardware (thermocouple input devices, NI, USB-9211, 4-Channel, 24-bit) under the Labview environment. Preliminary tests with five thermocouples located at different positions on the bottom of the Petri dish showed that the space variation of the sample temperature was very small, i.e. within 0.2 °C. The temperature variation of the thermocouple during the switch on period of the solar simulator was not detected, which indicated that the solar radiation didn't affect on the temperature acquiring inside nanofluid by the thermocouple. Sample fluid was injected slowly through a variable volume pipette into the Petri dish before each experiment.

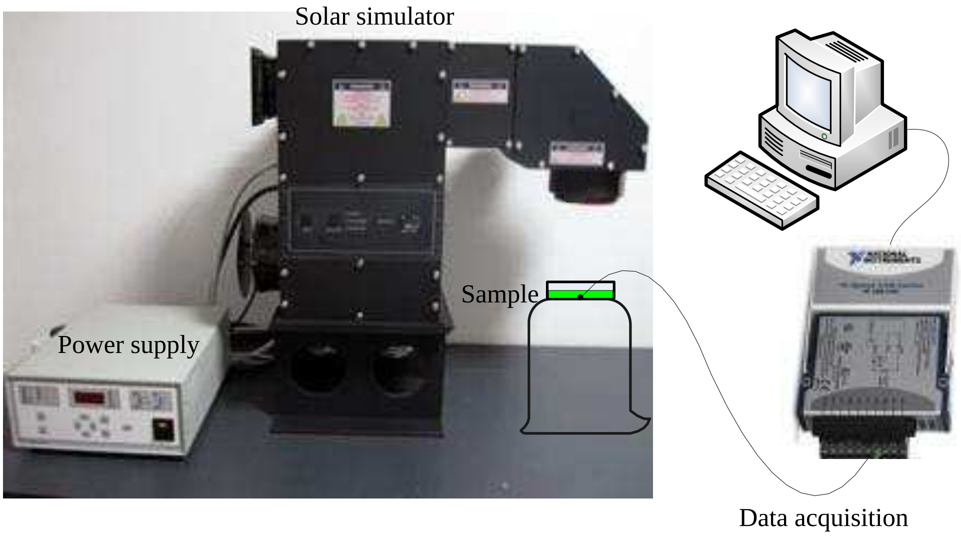

Fig. 3. Schematic of the experimental setup

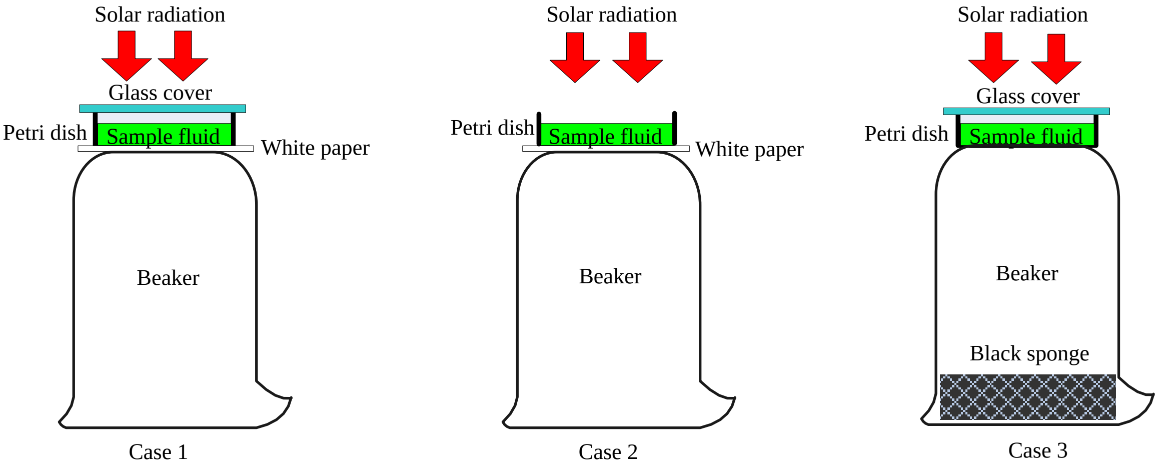

Fig. 4. Three cases in the experiment

The experiment was conducted for three cases, as shown in **Fig. 4**. For case 1, the Petri dish was covered by a glass plate (made of quartz glass, material type of JGS1, GiAi Photonics Corporation), which had high transparency from 185 nm to 2800 nm in spectrum. A piece of white paper was sandwiched between the Petri dish and the beaker; for case 2, the Petri dish was directly open to the ambient, and a piece of white paper was sandwiched between the Petri dish and the beaker; and for case 3, the Petri dish was covered by a glass plate, the white paper was removed, and a piece of black foam sponge was placed in the beaker to absorb the solar light transmitted through the sample fluid.

3. Numerical model

Aiming to investigate special absorbing properties for individual type and hybrids of nanofluids, a simulative model was built to predict the Absorption Efficiency (ABE). Through numerical model, the reason why hybrid nanofluids can enhance photothermal conversion efficiency and how to mix hybrid nanofluids properly can be comprehensively explained. Here we preferred to employ realistic solar irradiation profile based on ASTM G173-03 Reference Spectra [30], as shown in **Fig. 5.** Solar radiative power takes part of more than 95% in wavelength range between 200~3000 nm, but radiative power from nanofluids is mainly beyond 3000 nm, and is much small than that of sun, as can be seen in inset. So we separate the spectrum into two bands from 3000nm in order to simplify simulative model [31].

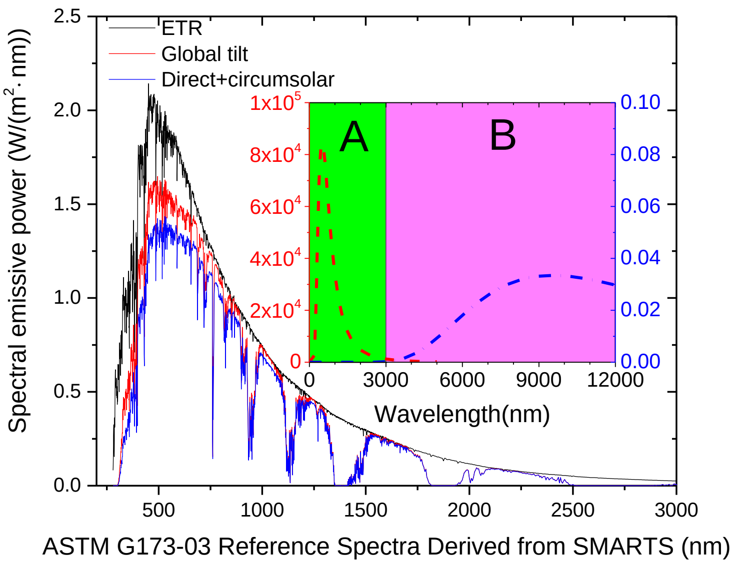

Fig. 5. ASTM G173-03 Reference Solar Spectra Emissive Power with wavelength, inset shows calculated spectral emissive power for sun (T=5762 K) and nanofluid (T=303 K), where spectral distribution is separated into two bands, A (λ<3000 nm) and B (λ > 3000 nm)

3.1 Mie scattering theory

In the present modeling, the characteristic size employed in radiative transfer equation is as $x_\lambda = \pi D / \lambda$, where D represents the diameter of nanoparticles. Since the diameter of suspended particles in the experiments are much smaller than the wavelength of irradiation (x_λ <<1), it is appropriate to use simplified equations, i.e., the Rayleigh scattering approximation [32] to calculate the absorption coefficient for nanofluids with small particle inside. However, in order to obtain detailed scattering parameters, such as the efficiencies for scattering, absorption, backscattering, averaged absolute-square E-field, the original Mie scattering equations [29] is preferred to identify the optical properties for spherical nanoparticle suspensions. The Mie scattering equations can be described by:

$$a_n = \frac{m\psi_n(mx)\psi_n'(x) - \psi_n(x)\psi_n'(mx)}{m\psi_n(mx)\xi_n'(x) - \xi_n(x)\psi_n'(mx)} \tag{2}$$

$$b_n = \frac{\psi_n(mx)\psi_n'(x) - m\psi_n(x)\psi_n'(mx)}{\psi_n(mx)\xi_n'(x) - m\xi_n(x)\psi_n'(mx)} \tag{3}$$

$$Q_{sca}(\lambda) = \frac{2}{x^2}\sum_{n=1}^{\infty}(2n+1)\left[|a_n|^2 + |b_n|^2\right] \tag{4}$$

$$Q_{ext}(\lambda) = \frac{2}{x^2}\sum_{n=1}^{\infty}(2n+1)\mathrm{Re}(a_n + b_n) \tag{5}$$

where the functions $\psi_n(x)$ and $\xi_n(x)$ are spherical Bessel functions[29] of order n (n= 1, 2,..) and the primes refer to the derivatives with respect to the argument, and m represents the ratio of refractive indexes, calculated by:

$$m = \frac{n_{particles}}{n_{fluid}} \tag{6}$$

where $n_{particles}$ and n_{fluid} are the complex refractive index [33–35] of particle material and based fluid (i.e. water) relative to the ambient medium, respectively. In consideration of relative low concentrations of nanofluids developed for solar thermal applications, particles should absorb and scatter light independently according to the scattering map [29]. With such a consideration, the absorption coefficient can be calculated from the below equation:

$$\kappa(\lambda)=\kappa_{p}(\lambda)+\kappa_{f}(\lambda)=\frac{3}{2}\frac{f_{v}Q_{abs}(\lambda)}{D}+\frac{4\pi k_{f}(\lambda)}{\lambda} \tag{7}$$

Here the particle of hybrid nanofluids we intend to investigate is in independent-scattering range[29], the absorption coefficient of hybrid nanofluids can be assumed as the summation of absorption of each kind of nanoparticles and the based fluid, which can be expressed as:

$$\begin{aligned}\kappa_{hybrid}(\lambda)&=\kappa_{Fe_3O_4}(\lambda)+\kappa_{Cu}(\lambda)+\kappa_{Au}(\lambda)+\kappa_{f}(\lambda)\\&=\frac{3}{2}\left[\left[\frac{f_{v}Q_{abs}(\lambda)}{D}\right]_{Fe_3O_4}+\left[\frac{f_{v}Q_{abs}(\lambda)}{D}\right]_{Cu}+\left[\frac{f_{v}Q_{abs}(\lambda)}{D}\right]_{Au}\right]+\frac{4\pi k_{f}(\lambda)}{\lambda}\end{aligned} \tag{8}$$

where the superscripts represent each type of nanofluids.

Based on Beer-Lambert Law [31], the absorbance can be obtained as:

$$\kappa(\lambda)\cdot L\cdot \log_{10} e=A(\lambda) \tag{9}$$

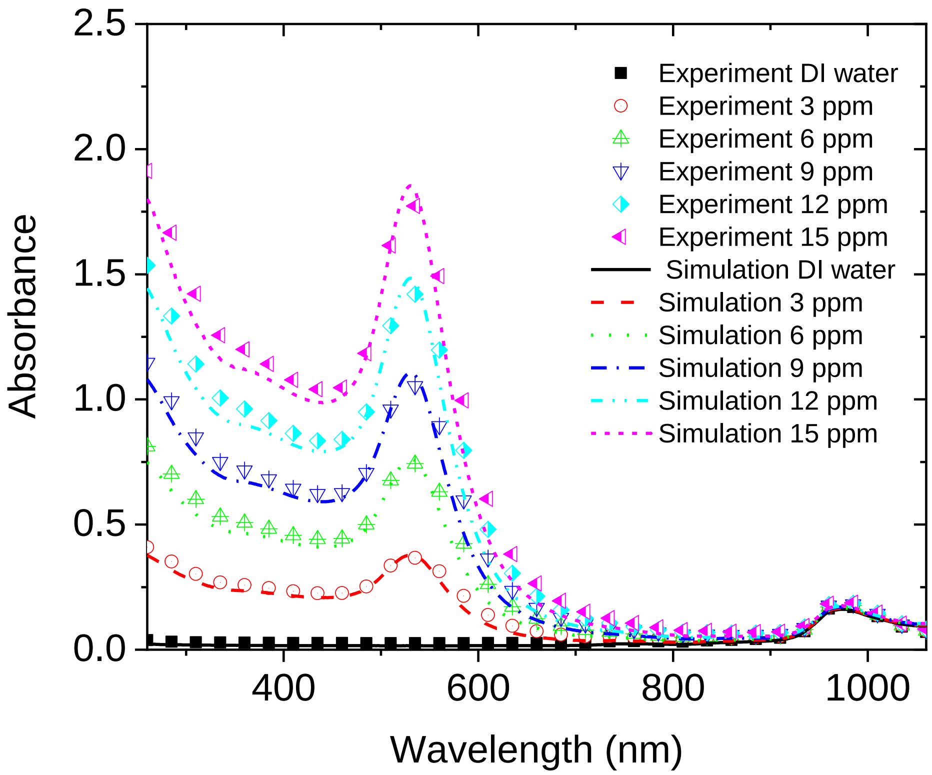

Fig. 6. Absorbance from UV spectral-photometer and simulation for gold nanofluids of different concentrations

Fig. 6 shows the comparison of simulative and experimental absorption from UV-spectrophotometer. As can be seen, results from Mie scattering theory are comparable with that from experiments. All samples exhibit very similar absorption curve shapes. The wavelength corresponds to the absorption peak is all about 520 nm, which is independent on the concentration of the nanofluids. Meanwhile the UV/Vis absorbance of Au nanofluids agrees pretty well with the Beer's law, i.e. the absorbance exhibits strict linear relation with the concentration. The proposed model can predict the absorbance for Fe_3O_4 and Cu nanofluid. However, due to the reactants and surfactant inside the fluid, the absorbance in UV region shows some infinity values (as shown in **Fig. 2**), which is not caused by nanoparticles. In this case, the model is not suitable to predict the absorbance in UV region. In order not to dilute the focal point of this work, the validation for Fe_3O_4 and Cu nanofluid is not presented.

3.2 **Predicted absorption efficiency**

As nanoparticle-based solar receiver, the solar energy absorption of nanoparticle can be simplified as 1-D radiative transfer, as shown in **Fig. 7**. The total absorption efficiency (ABE) can be described as [31]:

$$\eta(\mathrm{L},\ \mathrm{f_v})=\frac{\int_{0.2\mu m}^{3\mu m}\mathrm{E_0}(\lambda)\left(1-10^{-A(\lambda)\frac{L}{L_0}}\right)\mathrm{d}\lambda}{\int_{0.2\mu m}^{3\mu m}\mathrm{E_0}(\lambda)\,\mathrm{d}\lambda}=\frac{\int_{0.2\mu m}^{3\mu m}\mathrm{E_0}(\lambda)\left(1-e^{-\kappa(\lambda,\ f_v)L}\right)\mathrm{d}\lambda}{\int_{0.2\mu m}^{3\mu m}\mathrm{E_0}(\lambda)\,\mathrm{d}\lambda} \tag{10}$$

where the spectral wavelength for calculation is between 200 nm and 3000 nm, in which most of solar energy exists.

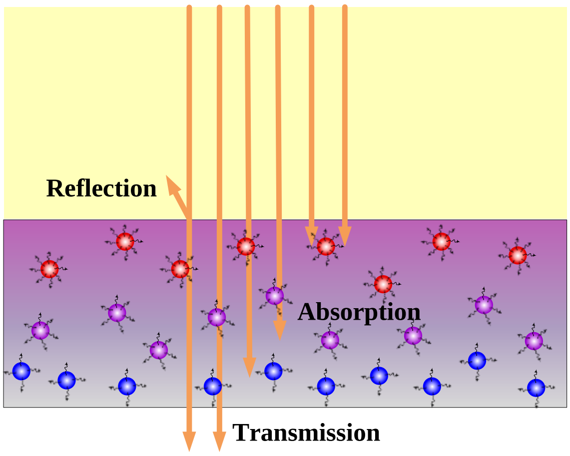

Fig. 7. Schematic absorption profiles in a nanoparticle-based solar receiver

Fe_3O_4, Cu and Au nanofluids with concentrations of 200 ppm, 50 ppm and 6 ppm were dispersed into each other with the same volume, respectively. The absorbance for each nanofluids and different hybrids can be seen in **Fig. 2**. These nanoparticle in such low concentration nanofluids should scatter light individually, as the size compared with the wavelength is in individual scattering range [29].Because two different nanofluids are dispersed into each other with the same volume concentration, the absorbance line in the whole spectrum of UV-spectrophotometer should go through the cross point of two individual absorbance lines (i.e. the absorbance lines for Cu, Au and Cu-Au hybrid nanofluids go through the same point at wavelength around 600 nm, as can be seen in **Fig. 2**), which is in consistent with Beer's Law. Hybrid nanofluid has the characteristics of mixed ingredients in absorbance, i.e., Au nanofluid and Cu nanofluid have absorbing peaks around 530 nm and 750 nm in wavelength, respectively. Obviously, hybrid nanofluid from Au and Cu has two identical peaks and exhibits more flat absorbance curve than that of Au or Cu nanofluid.

4. **Results and discussion**

4.1 **Effect of test conditions on solar energy absorption performance**

The solar energy absorption performance is influenced by not only the working fluids employed, but also the test conditions, and it is very important to understand the effect of different test conditions in the analysis of the experimental results. In this work, the experiment was first carried out in three cases to investigate the cover and reflection effects on the solar energy absorption performance.

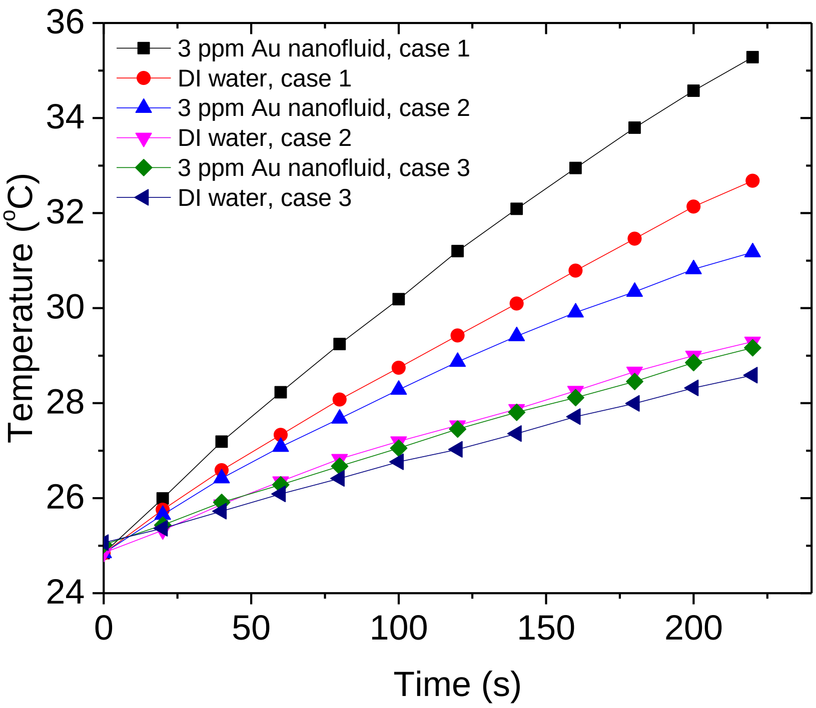

Fig. 8. Temperature variations of DI water and 3 ppm Au nanofluid in different cases

Fig. 8 shows the temperature variations of DI water and Au nanofluid with a concentration of 3 ppm in different cases. For a fixed solar radiation time of 220s in the same case, i.e., case 1 or 2, the temperature rise of Au nanofluid is obviously larger than that of DI water due to enhanced solar photothermal conversion performance of Au nanoparticles. However, more interestingly the glass cover plays an important role in affecting the temperature rise of the sample fluid. For DI water, the temperature rise is increased by 3.4°C when it is covered by a glass plate; and for Au nanofluid, the temperature rise is further increased by 4.0°C. The final temperature of DI water with a glass cover is even 1.5 °C higher than that of Au nanofluid without a glass cover, indicating that when the sample fluid is directly exposed to the ambient, as the fluid temperature rises continuously due to the absorption of solar radiation, the temperature difference between the sample fluid and the ambient increases gradually, and the heat loss from the sample fluid surface to the ambient through the evaporation and convection is comparatively large. The glass cover is made of quartz glass, which has high transparency from 185 nm to 2800 nm in spectrum. The glass cover will not affect the solar radiation. However, the glass cover will significantly absorb the long IR radiation form the nanofluid (above 4000 nm with the temperature of 303 K, as shown in **Fig. 5**), which prevents the radiative loss of nanofluid, the same phenomenon as the greenhouse effect. In order to avoid the influence of radiative and convective heat loss on the analysis of photothermal conversion efficiency, the glass cover is necessary for further experiment. By the employment of a glass cover, the heat loss to the ambient can be effectively inhibited, and it is very necessary to seal the sample fluid in later experiments to enhance the solar absorption performance.

As shown in **Fig. 8**, for a fixed solar radiation time of 220s in the same case, i.e., case 1 or 3, the temperature rise of Au nanofluid is obviously larger than that of DI water, due to enhanced solar photothermal conversion performance of Au nanoparticles. However, more interestingly the sunlight reflection plays an important role in affecting the temperature rise of the sample fluid. For DI water, the temperature rise is increased by 4.1°C when a piece of white paper is located under the Petri dish; and for Au nanofluid, the temperature rise is further increased by 6.0°C. That is because when a piece of white paper is located under the Petri dish, the sunlight penetrated through the sample fluid is reflected upwards, which will be absorbed by the sample fluid for two or even more times, resulting in a large temperature rise of the sample fluid. While when the white paper is removed, and a piece of black foam sponge is placed in the beaker, the sunlight will be absorbed by the sample fluid only once because most of the penetrated sun light will be absorbed by the black sponge, resulting in considerably reduced temperature rise of the sample fluid. To better characterize the solar energy absorption performance of the nanofluids investigated here, subsequent experiments will be always conducted in case 3, i.e., the sample fluid absorbs the sunlight only once with minimum heat loss to the surroundings.

4.2 Effect of different nanofluids on solar energy absorption performance

Fig. 9 shows a comparison of different working fluids on the solar energy absorption performance, including DI water, Fe_3O_4, Cu and Au nanofluids with different concentrations. As shown in **Fig. 9**, the solar energy absorption performance of Au nanofluid is the best, which is much better than that of Cu nanofluid. While for Fe_3O_4 nanofluid, the solar energy absorption performance is not favorable, which is only slightly better than that of DI water.

In fact, the solar photothermal conversion performance of a nanofluid depends on its solar spectral absorption property, which is directly influenced by the particle material, particle shape and morphology and the suspension concentration. Generally, the solar photothermal conversion performance of a nanofluid is more or less above that of the base fluid, i.e., DI water. That is because nanoparticles dispersed in the water have strong absorption of sunlight and the scattering effect between nanoparticles can also increase the optical path of photons entering the nanofluid, which is beneficial to the capture and absorption of sunlight.

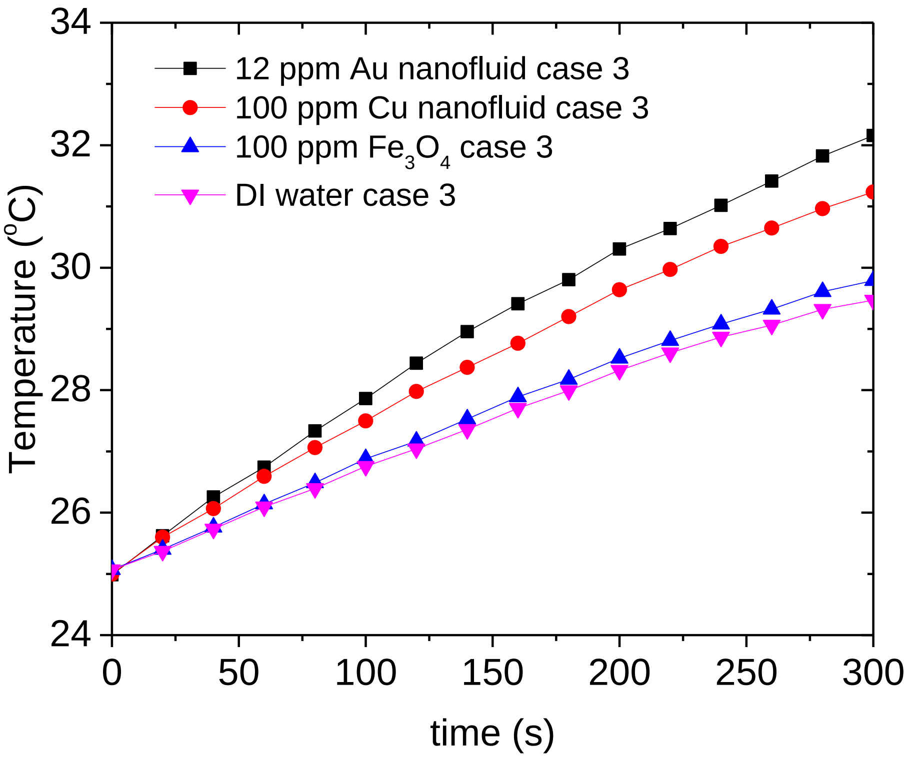

Fig. 9. Comparison of different nanofluids on solar energy absorption performance

Different from non-plasmonic materials, i.e., Fe_3O_4, for plasmonic materials such as Au, Ag and Cu nanoparticles, when the oscillation frequency of electrons in the metal is consistent with the incident light frequency, the plasmon resonance can be excited at the metal particle surface, and the absorption and scattering effects of sunlight can be significantly enhanced under the condition of resonance [36,37]. Therefore, at very low concentrations, the Au or Cu nanofluid exhibits much higher temperature rise compared to non-plasmonic materials.

4.3 **Nanoparticle concentration effect on solar energy absorption performance**

Fig. 10 shows the temperature variations of Au and Cu nanofluids with different concentrations in case 3, respectively. For both Au and Cu nanofluids, the higher the concentration, the larger the temperature rise of the nanofluids. For Au nanofluid, it is in good agreement with the UV-Vis absorbance results shown in **Fig. 6**, where a higher concentration corresponds to a larger solar absorbance.

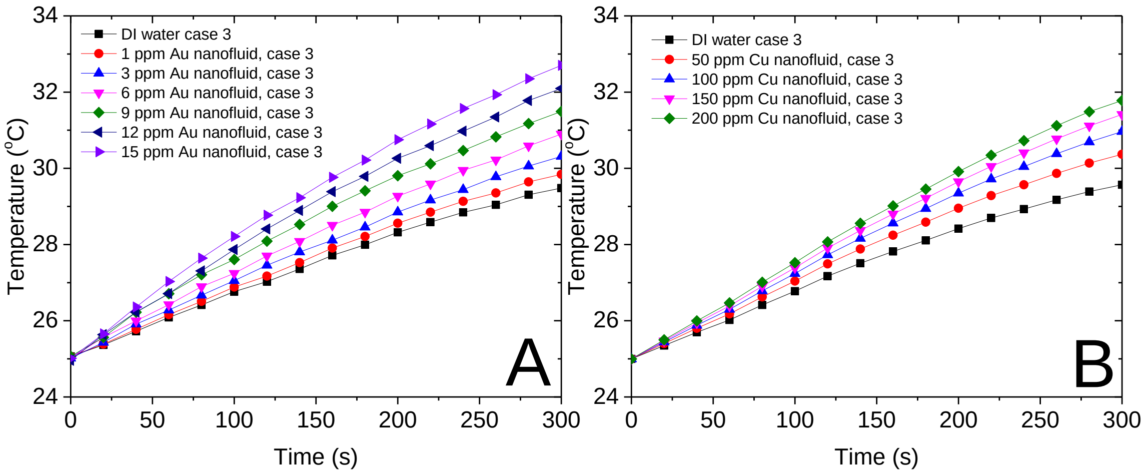

Fig. 10. Temperature variations with concentrations in case 3 of different nanofluids: (**A**) Au nanofluid; (**B**) Cu nanofluid

The absorption efficiency is conventionally defined as the ratio of the internal energy increase of the fluid to the total incident solar radiation:

$$\eta = \frac{(c_w m_w + c_n m_n)\Delta T}{I A \Delta t} \approx \frac{c_w m_w}{IA} \cdot \frac{\Delta \bar{T}}{\Delta t} \tag{11}$$

where $\Delta \bar{T}$ is the average temperature increase. Comparing with the base fluid, thermal energy stored in the nanoparticles is negligible owing to its low concentration and the heat capacity of the nanoparticles is usually lower than that of water. Here the total energy input from the solar simulator is used without considering the reflection from the glass tube. The evaporated water will re-condensate at the bottom of the glass cover, where the latent heat will release. This will trap the harvested heat absorbed from solar radiation. What's more, with the cover of the glass, the relative humidity inside the glass cover and the Petri dish will always be saturated, which can also prevent the evaporation of nanofluid to some extent. As analyzed above, the evaporative and convective heat loss is relatively small due to the glass cover (compared with case 1). It is rational not to involve the conventional definition of absorption efficiency, the same with our previous research [31,38]. Based on the standard error analysis method [39], the uncertainty for the photothermal conversion efficiency can be expressed as:

$$\frac{U_\eta}{\eta} = \sqrt{\left(\frac{U_T}{\Delta T}\right)^2 + \left(\frac{U_m}{m_w}\right)^2 + 2\left(\frac{U_D}{D_p}\right)^2 + \left(\frac{U_I}{I}\right)^2} \tag{12}$$

To quantify the capability of nanoparticles in absorbing solar energy, the specific absorption rate (SAR) is employed [18]:

$$SAR = \frac{(c_w m_w + c_n m_n)\Delta \bar{T}_n - c_w m_w \Delta \bar{T}_w}{m_n \Delta t} \quad (13)$$

The uncertainty for SAR can be expressed as:

$$U_{SAR} = U_T \sqrt{\left(\frac{c_w m_w + c_n m_n}{m_n \Delta t}\right)^2 + \left(\frac{c_w m_w}{m_n \Delta t}\right)^2} \quad (14)$$

where the uncertainty of mass of nanofluid was neglected due to the large difference between water mass and nanoparticle mass. The uncertainty analysis showed that the uncertainty of photothermal conversion efficiency and SAR were within 1%. All the experiments were performed 3 times and the results showed that the uncertainty was within 3%.

Fig. 11 shows the variation of the solar energy absorption efficiency of Au and Cu nanofluids with different concentrations in case 3, respectively. For both Au and Cu nanofluids, the higher the concentration, the larger the solar energy absorption efficiency of the nanofluids. However, the increasing rate of the absorption efficiency slows down gradually with the increase of the concentration of the nanofluids. This is consistent to the Beer's law where a logarithm relation exists between the transmittance and the concentration of the nanofluids. For DI water, the solar energy absorption efficiency is 20.3%, while it is increased up to 34.3% and 30.2% for 15.0 ppm Au nanofluid and 210 ppm Cu nanofluid respectively, indicating that the addition of a very little amount of nanoparticles into the base fluid, i.e. water, can significantly enhance the solar energy absorption performance.

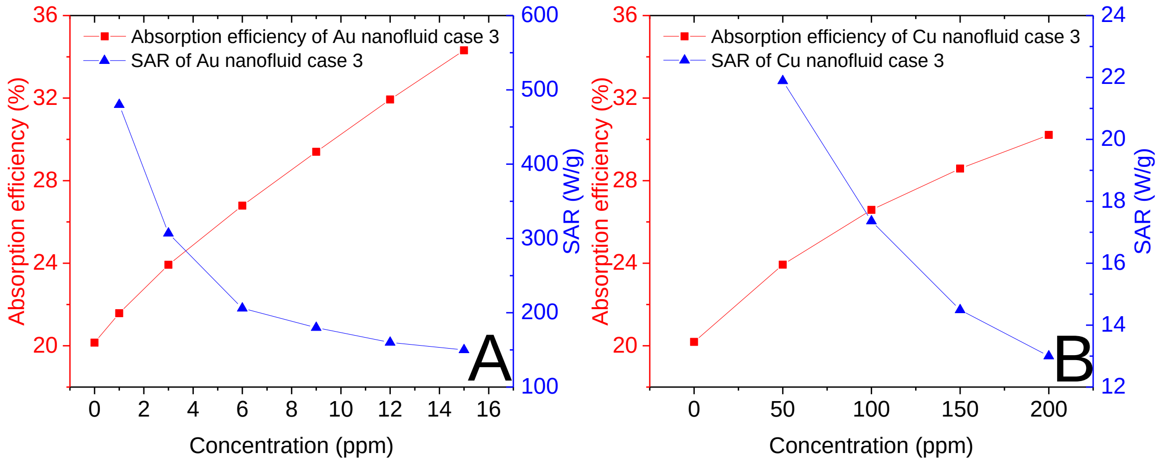

Fig. 11. Variation of solar energy absorption efficiency and SAR with different concentrations of (**A**) Au nanofluid and (**B**) Cu nanofluid

At the same concentration, the solar energy absorption efficiency of Au nanofluid is much higher than that of Cu nanofluid. For instance, when the concentration is 10 ppm, the solar energy absorption efficiency of Cu nanofluid is about 21%, whereas for Au nanofluid, it can be increased up to 31%. This is because Au nanoparticles have a much stronger effect of localized surface plasmon resonance compared to Cu nanoparticles, which leads to a much better solar photothermal conversion performance.

Fig. 11 also shows the variation of the SAR of Au and Cu nanoparticles with different concentrations in case 3, respectively. For both Au and Cu nanofluids, the SAR decreases gradually with the increase of the concentration; at the same time, the SAR of Au nanoparticles is much higher than that of the Cu nanoparticles in the experiments. Clearly, the SAR is proportional to the difference of the temperature increase rate between the nanofluid and the base fluid. The overall effects result in the unique variation of the SAR of different nanoparticles.

4.4 **Solar energy absorption performance of hybrid nanofluids**

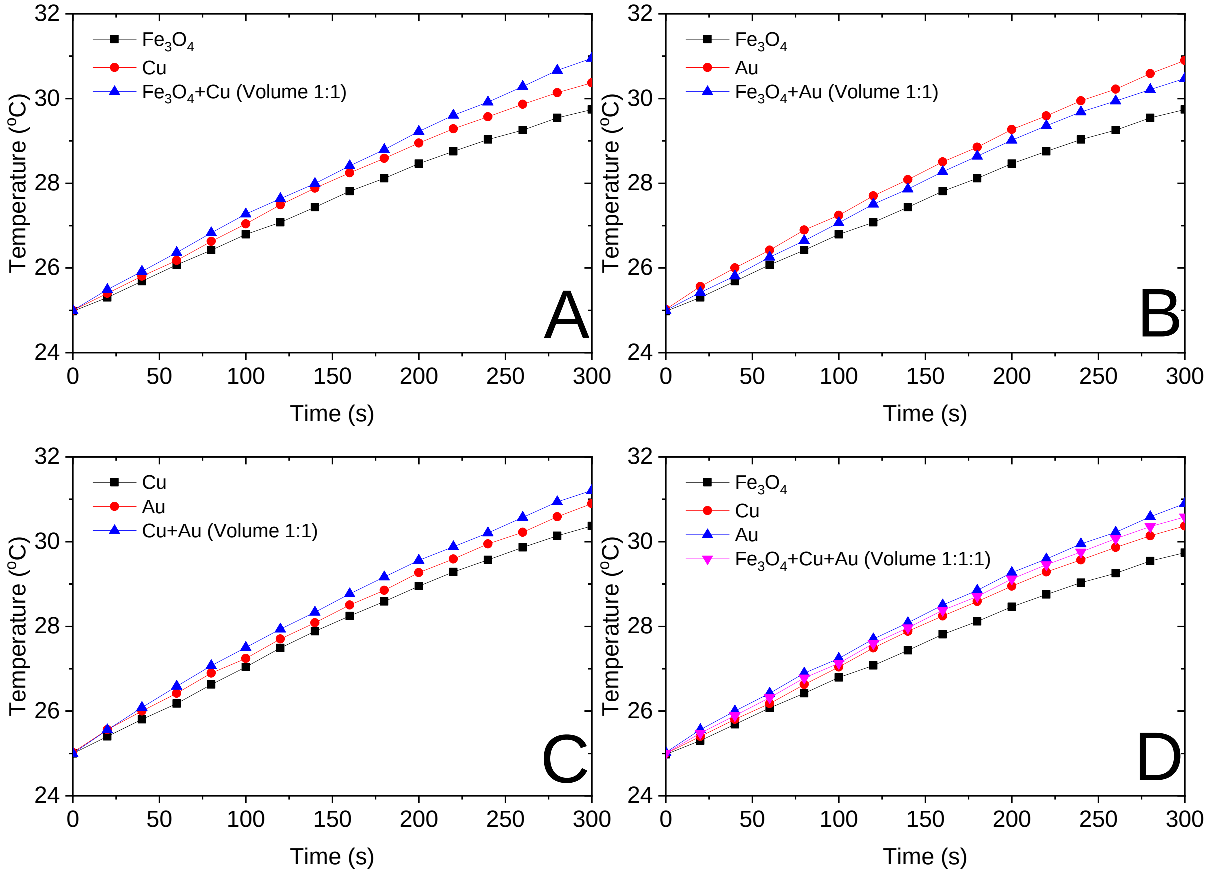

Fig. 12. Temperature variations of hybrid nanofluids in case 3

As introduced in section 2.1, the hybrid nanofluids were prepared using the same volume of Fe_3O_4, Cu and Au nanofluid with concentration of 200 ppm, 50 ppm and 6 ppm, respectively. The photothermal conversion performance of hybrid nanofluids can be seen in **Fig. 12**. The temperature variations of Fe_3O_4+Cu hybrid nanofluid with different concentrations are shown in **Fig. 12A**. The temperature increase of Fe_3O_4+Cu hybrid nanofluid is higher than that of Fe_3O_4 nanofluid or Cu nanofluid. The same thing happens with Cu and Au hybrid nanofluid, as shown in **Fig. 12C**, i.e., the temperature of Cu+Au hybrid nanofluid is 31.2 ℃, higher that of Cu or Au nanofluid (which are 30.36 ℃ and 30.89 ℃ at 300 s, respectively). The simple mixing of Fe_3O_4 and Cu nanofluids, or the mixing of Cu and Au nanofluid can gain extra benefit when absorbing solar energy. However, the temperature of Fe_3O_4, Au and Fe_3O_4+Au nanofluid are 29.74 ℃, 30.89 ℃ and 30.47 ℃, respectively, which means the mixing of Fe_3O_4 and Au nanofluid will not gain the extra benefit, as shown in **Fig. 12B**. Simply mixing Fe_3O_4, Cu and Au nanofluid, i.e., the Fe_3O_4+Cu+Au does not have higher absorption efficiency than that of individual nanofluid, as shown in **Fig. 12D**.

Due to the localized surface plasmon resonance effect, Au nanofluids exhibit excellent absorption performance of solar thermal energy compared to nanofluids with non-plasmonic nanomaterials, such as oxide nanofluids. However, for Au nanoparticles, the wavelength corresponds to its solar absorption peak is around 520 nm, as shown in **Fig. 2**, and its absorption capability becomes worse for the sunlight with the wavelength larger than 600 nm. It is possible to further enhance the absorption of sunlight with the wavelength larger than 600 nm by simply increasing the concentration of Au nanofluid; however, it is obviously not an economical way, taking into account the high cost of gold material. While for Cu nanoparticles, the wavelength corresponds to its solar absorption peak is larger than 700 nm, and it is a novel idea to combine Au and Cu nanofluids to improve the solar absorption in the whole solar visible spectrum (390-760 nm), as verified by **Fig. 2** where the solar visible light absorbance is evidently enhanced by the Cu-Au hybrid nanofluid compared with Au nanofluid at the same Au nanoparticle concentration. This indicates that the application of the hybrid nanofluids to further enhance the solar energy absorption efficiency should be a practically feasible and cost-effective method. The same thing happens when considering about Fe_3O_4 and Cu nanofluid. Because they have different absorption peaks in spectrum, the Fe_3O_4+Cu hybrid nanofluid has higher absorption efficiency than that of individual nanofluid. Further investigation will be discussed in the next section.

4.5 Efficiency enhancement from hybrid nanofluids

In order to investigate whether hybrid nanofluid can enhance photothermal conversion efficiency, Eq. 10 was calculated with optical depth from 0.001 m to 0.03 m for all nanofluids we tested in this paper, as shown in **Fig. 13**.

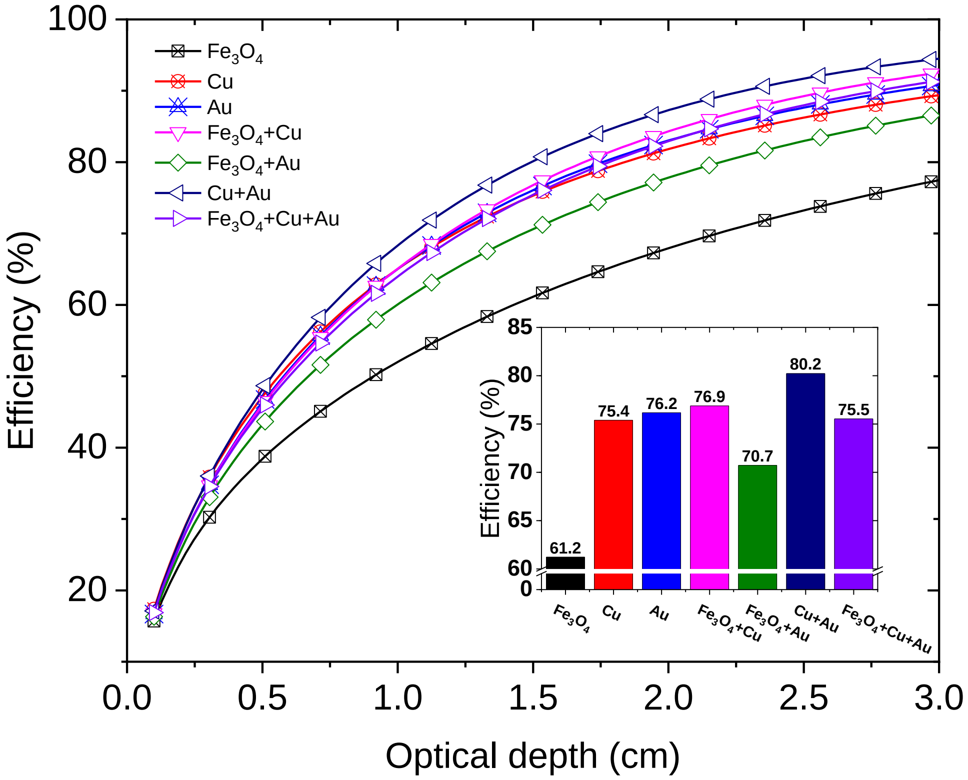

Fig. 13 Predicted efficiency for single nanofluids and hybrids with changing optical depth, inset shows photothermal conversion efficiency when optical depth is 0.015 m

Results from can be concluded as:

1) Photothermal conversion efficiency increases with optical depth for all nanofluids, which is in consistent with our previous research [18,26,31,38]

2) For all nanofluids, Cu-Au hybrid nanofluid exhibits highest efficiency while Fe_3O_4 nanofluid exhibits lowest efficiency

3) If two nanofluids with distinct absorbing peak in spectrum, their hybrid nanofluid could possibly exhibit higher absorbing efficiency when mixing with each other with equal radio than that of single nanofluid, i.e., Au and Cu nanofluid have absorbing peak around 531 nm and 750 nm, respectively, and they have efficiency about 76% and 75%; after mixed with each other to become a hybrid, higher efficiency as much as 80% is reached. The same mechanism happens with Cu and Fe_3O_4

4) However, if two nanofluid share similar absorbing behavior in spectrum (i.e., Au and Fe_3O_4 have higher absorbing efficiency in UV range but lower efficiency in near-infrared range, as can be seen in **Fig. 2**), it is possible to get a lower efficiency if mixing them together to become a hybrid

If hybrid nanofluids could enhance photothermal conversion efficiency by just mixing two kind of nanofluids with different advantaged absorbing peak spectrum, it is very interesting to investigate that at what volume fraction when two kinds of nanofluids mixing into each other will reach the maximum absorbing efficiency. According to Beer's Law and Eq. 9, predicted efficiency changing with mixing volume fraction at optical depth of 0.015 m (a typical value) can be seen in **Fig. 14**. For Cu+Au hybrid nanofluids, a peak efficiency of 80.1% occurs when volume fraction of Au nanofluid is 0.516 (the volume of Au takes 51.6% in the mixed hybrid nanofluid). As much as 76.2% of efficiency can be reached when volume fraction of Cu nanofluid is 0.788 in Fe_3O_4+Cu hybrid nanofluid. However, for Fe_3O_4+Au nanofluid, absorbing efficiency increases monotonously with increasing of Au nanofluid's volume fraction.

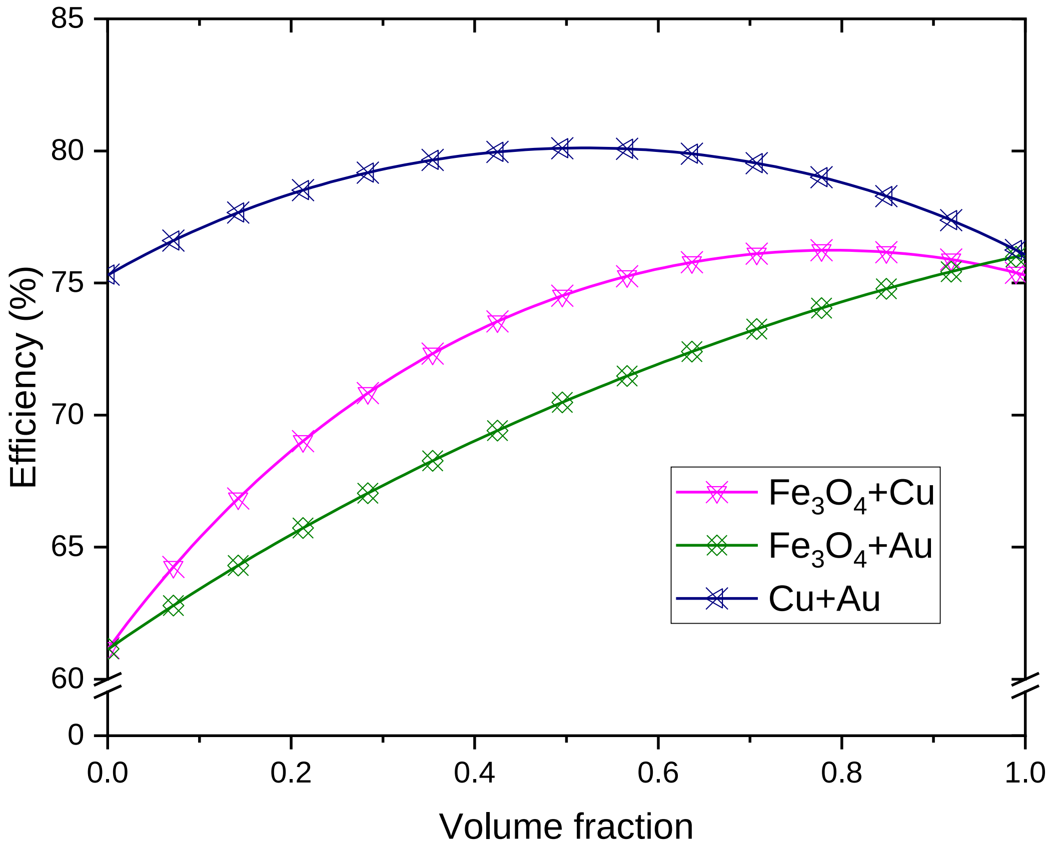

Fig. 14 Predicted photothermal conversion efficiency from numerical model for hybrid nanofluids with changing volume fraction of mixing ingredient when optical depth is 0.015 m

In the present study, the calculation of the solar photothermal conversion efficiency η and the specific absorption rate SAR of the nanofluids are conducted in a very simple way, although it can reasonably reflect the major variation trends of these variables. There are still some factors that should be taken into account in the later research. In our previous research [31,38], ununiform temperature distribution was found when nanofluid under concentrated solar radiation. In this paper, the temperature distribution of the nanofluid may not be very uniform, and the one-point measurement of the temperature cannot precisely represent the average temperature of the nanofluid, although the maximum temperature difference within the nanofluid should be not large for the present experimental condition. Actually, the ununiform temperature distribution is closely related to the optical depth, i.e., the thickness of the petri dish. Furthermore, the solar photothermal conversion characteristics of each nanoparticle should be different at different locations especially along the thickness direction.

This work has validated the novel idea of employing hybrid nanofluids to effectively enhance the solar absorption efficiency; however, it is still at the early stage of the research, i.e., only certain concentration of the Fe_3O_4, Cu and Au nanoparticles are mixed and studied experimentally. Numerical study indicates that the optimal volume fraction of nanofluid should play important roles when absorbing solar energy. Future studies should focus on optimization of the concentration and volume of hybrid nanofluids in order to reach a trade-off between the cost effectiveness and solar absorption performance. In addition, hybrid nanofluids composed of other nanoparticles such as silver, iron oxide and single or multiple-walled carbon nanotube nanomaterials should be considered, and different methods to synthesize more stable hybrid nanofluids should be explored and developed. At last, for the present study, the nanofluids investigated are always in the quiescent condition, and it is of great importance to investigate the solar absorption performance of different nanofluids including the hybrid nanofluids under flow condition, which is much similar to the situation in most practical engineering applications.

5. Conclusions

In order to enhance the solar photothermal conversion performance based on the direct absorption concept, Fe_3O_4, Cu and Au nanofluid with different concentrations and hybrid nanofluids were prepared and characterized in this work. Extensive experiments were conducted with different nanofluids under a solar simulator. A numerical method to predict solar absorption efficiency has been proposed to investigate the roles of nanoparticles for hybrid nanofluid, and important conclusions have been drawn and summarized as follows:

1) The test conditions significantly affect the solar absorption performance of the sample nanofluid by comparing the experimental results in three cases, and the test condition where the simulated sunlight is absorbed by the sample nanofluid only once with minimum heat loss to the surroundings is determined;

2) The solar energy absorption performance of nanofluids with plasmonic nanomaterials, i.e., Au or Cu, is much better than that of nanofluids with non-plasmonic nanomaterials, i.e., Fe_3O_4 and DI water, due to the effect of localized surface plasmon resonance;

3) The larger the concentration, the higher the solar energy absorption efficiency, whereas the increasing rate of the absorption efficiency slows down gradually with the increase of the concentration;

4) The solar energy absorption efficiency and specific absorption rate (SAR) of Au nanofluid are much larger than those of Cu nanofluid, because the Au nanofluid has a much stronger effect of the localized surface plasmon resonance, but the wavelengths correspond to their solar absorption peaks are much different;

5) The novel idea of employing hybrid nanofluid to improve the solar absorption performance has been experimentally and numerically validated, which can enhance the solar photothermal conversion when mixing two nanofluids with different absorption peaks. There is an optimal mixing volume fraction for hybrid nanofluid. Further investigation should be focused on the roles of concentration and volume of hybrids for solar thermal harvesting.

Acknowledgement

This work was supported by the National Natural Science Foundation of China (No.51776012 and No.51306009) and the EU Marie Curie Actions-International Incoming Fellowships (FP7-PEOPLE-2013-IIF-626576). The author Haichuan Jin also acknowledges the financial support for his visiting study at the University of Leeds from the China Scholarship Council (CSC) under the Grant No.201506020031.

Reference

[1] M. Chen, Y. He, J. Zhu, Y. Shuai, B. Jiang, Y. Huang, An experimental investigation on sunlight absorption characteristics of silver nanofluids, Sol. Energy. 115 (2015) 85–94. doi:10.1016/j.solener.2015.01.031.

[2] T.P. Otanicar, P.E. Phelan, J.S. Golden, Optical properties of liquids for direct absorption solar thermal energy systems, Sol. Energy. 83 (2009) 969–977. doi:10.1016/j.solener.2008.12.009.

[3] S. Vijayaraghavan, S. Ganapathisubbu, C. Santosh Kumar, Performance analysis of a spectrally selective concentrating direct absorption collector, Sol. Energy. 97 (2013) 418–425. doi:10.1016/j.solener.2013.08.008.

[4] Y. Gan, L. Qiao, Optical properties and radiation-enhanced evaporation of nanofluid fuels containing carbon-based nanostructures, Energy and Fuels. 26 (2012) 4224–4230. doi:10.1021/ef300493m.

[5] H. Tyagi, P. Phelan, R. Prasher, Predicted Efficiency of a Nanofluid-Based Direct Absorption Solar Receiver, ASME 2007 Energy Sustain. Conf. (2007) 729–736. doi:10.1115/ES2007-36139.

[6] T. Yousefi, E. Shojaeizadeh, F. Veysi, S. Zinadini, An experimental investigation on the effect of pH variation of MWCNT-H2O nanofluid on the efficiency of a flat-plate solar collector, Sol. Energy. 86 (2012) 771–779. doi:10.1016/j.solener.2011.12.003.

[7] T. Yousefi, F. Veysi, E. Shojaeizadeh, S. Zinadini, An experimental investigation on the effect of Al 2O 3-H 2O nanofluid on the efficiency of flat-plate solar collectors, Renew. Energy. 39 (2012) 293–298. doi:10.1016/j.renene.2011.08.056.

[8] S.K. Verma, A.K. Tiwari, Progress of nanofluid application in solar collectors: A review, Energy Convers. Manag. 100 (2015) 324–346. doi:10.1016/j.enconman.2015.04.071.

[9] A. Kasaeian, A.T. Eshghi, M. Sameti, A review on the applications of nanofluids in solar energy systems, Renew. Sustain. Energy Rev. 43 (2015) 584–598. doi:10.1016/j.rser.2014.11.020.

[10] B. Tang, Y. Wang, M. Qiu, S. Zhang, A full-band sunlight-driven carbon nanotube/PEG/SiO2 composites for solar energy storage, Sol. Energy Mater. Sol. Cells. 123 (2014) 7–12. doi:10.1016/j.solmat.2013.12.022.

[11] A. Lenert, E.N. Wang, Optimization of nanofluid volumetric receivers for solar thermal energy conversion, Sol. Energy. 86 (2012) 253–265. doi:10.1016/j.solener.2011.09.029.

[12] R. Kandasamy, I. Muhaimin, A.K. Rosmila, The performance evaluation of unsteady MHD non-Darcy nanofluid flow over a porous wedge due to renewable (solar) energy, Renew. Energy. 64 (2014) 1–9. doi:10.1016/j.renene.2013.10.019.

[13] A. Zeiny, H. Jin, G. Lin, P. Song, D. Wen, Solar evaporation via nanofluids: A comparative study, Renew. Energy. 122 (2018) 443–454. doi:10.1016/j.renene.2018.01.043.

[14] S. Delfani, M. Karami, M.A. Akhavan-Behabadi, Performance characteristics of a residential-type direct absorption solar collector using MWCNT nanofluid, Renew. Energy. 87 (2016) 754–764. doi:10.1016/j.renene.2015.11.004.

[15] T.P. Otanicar, P.E. Phelan, R.S. Prasher, G. Rosengarten, R.A. Taylor, Nanofluid-based direct absorption solar collector, J. Renew. Sustain. Energy. 2 (2010). doi:10.1063/1.3429737.

[16] M. Karami, M.A. Akhavan Bahabadi, S. Delfani, A. Ghozatloo, A new application of carbon nanotubes nanofluid as working fluid of low-temperature direct absorption solar collector, Sol. Energy Mater. Sol. Cells. 121 (2014) 114–118. doi:10.1016/j.solmat.2013.11.004.

[17] H. Zhang, H.J. Chen, X. Du, D. Wen, Photothermal conversion characteristics of gold nanoparticle dispersions, Sol. Energy. 100 (2014) 141–147. doi:10.1016/j.solener.2013.12.004.

[18] F.E.P. Bandarra, O.S.H. Mendoza, C.L.L. Beicker, A. Menezes, D. Wen, Experimental investigation of a silver nanoparticle-based direct absorption solar thermal system, Energy Convers. Manag. 84 (2014) 261–267. doi:10.1016/j.enconman.2014.04.009.

[19] Q. He, S. Wang, S. Zeng, Z. Zheng, Experimental investigation on photothermal properties of nanofluids for direct absorption solar thermal energy systems, Energy Convers. Manag. 73 (2013) 150–157. doi:10.1016/j.enconman.2013.04.019.

[20] V. Khullar, H. Tyagi, N. Hordy, T.P. Otanicar, Y. Hewakuruppu, P. Modi, R.A. Taylor, Harvesting solar thermal energy through nanofluid-based volumetric absorption systems, Int. J. Heat Mass Transf. 77 (2014) 377–384. doi:10.1016/j.ijheatmasstransfer.2014.05.023.

[21] H. Zhang, H.-J. Chen, X. Du, G. Lin, D. Wen, Dependence of Photothermal Conversion Characteristics on Different Nanoparticle Dispersions, J. Nanosci. Nanotechnol. 15 (2015) 3055–3060. doi:10.1166/jnn.2015.9673.

[22] S.M. Ladjevardi, A. Asnaghi, P.S. Izadkhast, A.H. Kashani, Applicability of graphite nanofluids in direct solar energy absorption, Sol. Energy. 94 (2013) 327–334. doi:10.1016/j.solener.2013.05.012.

[23] Z. Luo, C. Wang, W. Wei, G. Xiao, M. Ni, Performance improvement of a nanofluid solar collector based on direct absorption collection (DAC) concepts, Int. J. Heat Mass Transf. 75 (2014) 262–271. doi:10.1016/j.ijheatmasstransfer.2014.03.072.

[24] R. Massart, Preparation of Aqueous Magnetic Liquids in Alkaline and Acidic Media, IEEE Trans. Magn. 17 (1981) 1247–1248. doi:10.1109/TMAG.1981.1061188.

[25] A. Zeiny, H. Jin, L. Bai, G. Lin, D. Wen, A comparative study of direct absorption nanofluids for solar thermal applications, Sol. Energy. 161 (2018) 74–82. doi:10.1016/j.solener.2017.12.037.

[26] H. Zhang, H.J. Chen, X. Du, D. Wen, Photothermal conversion characteristics of gold nanoparticle dispersions, Sol. Energy. 100 (2014) 141–147. doi:10.1016/j.solener.2013.12.004.

[27] T.P. Otanicar, P.E. Phelan, R.S. Prasher, G. Rosengarten, R.A. Taylor, Nanofluid-based direct absorption solar collector, J. Renew. Sustain. Energy. 2 (2010) 033102. doi:10.1063/1.3429737.

[28] E. Sani, L. Mercatelli, S. Barison, C. Pagura, F. Agresti, L. Colla, P. Sansoni, Potential of carbon nanohorn-based suspensions for solar thermal collectors, Sol. Energy Mater. Sol. Cells. 95 (2011) 2994–3000. doi:10.1016/j.solmat.2011.06.011.

[29] M.F. Modest, Radiative Heat Transfer, Academic Press, 2003. doi:http://dx.doi.org/10.1016/B978-012503163-9/50021-7.

[30] C.A. Gueymard, The sun’s total and spectral irradiance for solar energy applications and solar radiation models, Sol. Energy. 76 (2004) 423–453. doi:10.1016/j.solener.2003.08.039.

[31] H. Jin, G. Lin, L. Bai, M. Amjad, E.P. Bandarra Filho, D. Wen, Photothermal conversion efficiency of nanofluids: An experimental and numerical study, Sol. Energy. 139 (2016) 278–289. doi:10.1016/j.solener.2016.09.021.

[32] T. Moore, ABSORPTION AND SCATTERING OF LIGHT BY SMALL PARTICLES by C.F. Bohren and D.R. Huffman, Wiley Science Paperback Series, Chichester, UK, 1998, xiv+530 pp., List of references, index (£34.95; pbk)., John Wiley & Sons, 1998. doi:10.1017/S0263574798270858.

[33] K.M. McPeak, S. V. Jayanti, S.J.P. Kress, S. Meyer, S. Iotti, A. Rossinelli, D.J. Norris, Plasmonic films can easily be better: Rules and recipes, ACS Photonics. 2 (2015) 326–333. doi:10.1021/ph5004237.

[34] S. Babar, J.H. Weaver, Optical constants of Cu, Ag, and Au revisited, Appl. Opt. 54 (2015) 477. doi:10.1364/AO.54.000477.

[35] G.M. Hale, M.R. Querry, Optical Constants of Water in the 200-nm to 200-μm Wavelength Region, Appl. Opt. 12 (1973) 555. doi:10.1364/AO.12.000555.

[36] S.A. Maier, Plasmonics: Fundamentals and applications, Plasmon. Fundam. Appl. (2007) 1–223. doi:10.1007/0-387-37825-1.

[37] C. Noguez, Surface plasmons on metal nanoparticles: The influence of shape and physical environment, J. Phys. Chem. C. 111 (2007) 3606–3619. doi:10.1021/jp066539m.

[38] H. Jin, G. Lin, L. Bai, A. Zeiny, D. Wen, Steam generation in a nanoparticle-based solar receiver, Nano Energy. 28 (2016) 397–406. doi:10.1016/j.nanoen.2016.08.011.

[39] R.J. Moffat, Describing the uncertainties in experimental results, Exp. Therm. Fluid Sci. 1 (1988) 3–17. doi:10.1016/0894-1777(88)90043-X.